Supporting Information for

Metal Monophosphonates $M\{(2\text{-}C_5H_4NO)CH_2PO_3\}(H_2O)_2$ (M = Co, Ni, Mn, Cd): Synthesis, Structure, and Magnetism

Ting-Hai Yang,[a] Elisabeth S. Knowles,[b] Daniel M. Pajerowski,[b] Jian-Sheng Xia,[b] Liang Yin,[b] Song Gao,[c] Mark W. Meisel,[b,*] Li-Min Zheng [a,*]

[a] State Key Laboratory of Coordination Chemistry, School of Chemistry and Chemical Engineering, Nanjing University, Nanjing 210093, P. R. China

[b] Department of Physics and the National High Magnetic Field Laboratory, University of Florida, Gainesville, Florida 32611-8440, USA

[c] Beijing National Laboratory for Molecular Sciences, College of Chemistry and Molecular Engineering, Peking University, Beijing 100871, P. R. China

E-mail: lmzheng@nju.edu.cn and meisel@phys.ufl.edu

Abstract

This supporting information describes: (A) the details of the low temperature, high field measurements, while also providing additional data; and (B) the analysis of the high temperature, low field data that was acquired in Nanjing and in Gainesville; and (C) the high temperature dc and ac susceptibility of **1**.

A. Low temperature, high field measurements

General Procedure for 1 and 2. Similar to previous work [1], the magnetic susceptibility studies were performed with ac mutual inductance coils mounted on a dilution refrigerator equipped with a 10 T magnet. With the sample immersed in pure ^{3}He that provided intimate thermal contact with the mixing chamber, the in-phase and out-of-phase signals of the susceptibility were recorded by a two channel lock-in amplifier. Various frequencies, ranging from 24.7 Hz to 555 Hz, were used to search for an optimal response, and the ac field was nominally 0.1 mT. Typically the data were obtained by isothermal field sweeps at a rate of 50 mT/min, which is a rate that provides reversible results and avoids heating. For the Co and Ni samples, the data were independent of the direction of the field sweep. In each case, a sample mass of approximately 25 mg was used.

In parallel, specimens from the same batch of materials used for the low temperature studies were measured in a commercial SQUID magnetometer at 2 K and in fields up to 7 T. These results were consistent with the ones reported to us from the Nanjing Group, as described later.

General Procedure for 3. See preceding paragraph for some details. At 84.7 Hz and 50 mK, a sweep up to and down from 10 T was made, and significant hysteresis was observed for the first time in any measurements made on this instrument. Next, at 84.7 Hz, field sweeps were then performed at 50 mK, 150 mK, 600 mK, 900 mK, 2 K, 4 K (a), 3 K, 4 K (b) (note repeat at this temperature), and 5.5 K. At 5.5 K and in a field near 8 T, a dramatic signal change was assigned to the superconducting to normal transition of the primary coil. Typical sweep rates of 5 T per 100 min were used, although several other rates were checked.

A sample mass of approximately 25 mg was used, but it is important to note that the Mn sample is really small parallelpiped microcrystals, whereas the Co and Ni samples were more powder-like, consisting of irregularly shaped spheres.

In parallel, specimens from the same batch of materials used for the low temperature studies were measured in a commercial SQUID magnetometer at 2 K and in fields up to 7 T. These results were consistent with the ones reported to us from the Nanjing Group, as described later.

Samples. All magnetic measurements in Gainesville were performed on powder-like samples of each compound. Compound **1** was a reddish powder-like sample composed of irregular spheres with diameters ranging from 100 to 500 μm. Compound **2** was a greenish powder-like sample composed of irregular spheres with diameters of approximately 100 μm. Compound **3** was composed of small dark-yellowish parallelepiped micro-crystals with lengths ranging from 400 to 900 μm and widths spanning from 100 to 200 μm.

Analysis. In previous work [1], the low temperature and high field signals allowed for a background to be determined, since the sample achieved full saturation and the signal was strong. However, for the present work, whenever this procedure was attempted, the magnetic field dependence of the treated data was highly dependent on the subtraction protocol. Consequently, the magnitude of the ac voltage (= $\{\text{in-phase}^2 + \text{out-of-phase}^2\}^{1/2}$) was analyzed without any background subtractions. This response, dM/dB, where M is the magnetization of the sample and B is the applied magnetic field, was differentiated to obtain d^2M/dB^2, which is plotted versus B in the plots. Ultimately, the shape of the response is complicated by the background arising from the measuring coils, and as of March 2010, a different set of coils are being developed for future measurements.

Data. The data for compounds **1**, **2**, and **3** are given Figures S1, S2, and S3, respectively. The figure captions and legends provide information about the frequencies that were employed. The magnetic field axes are limited to the regions where the temperature dependent features were observed. For **1** and **2**, no other signatures that could be assigned to the samples were observed at higher magnetic fields, although the sweeps were typically made to full field, 10 T. For **3**, the hysteresis was interpreted as the physical realignment, after B_{sat} was achieved, of part of the sample that had not been fully immobilized.

B. High temperature, low field analysis and data

Taking the dimer Hamiltonian as $H = -J\, S_A \cdot S_B$, the equation for the dimer susceptibility is [2]

$$\chi_{Dimer}(T) = \frac{Ng^2\mu_B^2}{3k_BT} \cdot \frac{\sum_{S=0}^{2S_A} S(S+1)(2S+1)\exp[\frac{1}{2}S(S+1)\frac{J}{k_BT}]}{\sum_{S=0}^{2S_A}(2S+1)\exp[\frac{1}{2}S(S+1)\frac{J}{k_BT}]} \quad . \qquad \text{(S1)}$$

Incorporating a weak inter-dimer interaction, J', in the molecular field approximation, as well as a fraction of unpaired spins, ρ, and a temperature-independent background susceptibility, χ_o, the equation for the total susceptibility of the sample can be written as

$$\chi(T) = \frac{\chi_{Dimer}}{1 - \frac{2zJ'}{Ng^2\mu_B^2}\cdot\chi_{Dimer}} + \rho\frac{2Ng^2\mu_B^2 S(S+1)}{3k_BT} + \chi_o \quad . \qquad \text{(S2)}$$

New fits were performed at UF on the χT data from for compounds **2** and **3** using Equation S2, with g, J, zJ', and ρ as parameters. For compound **1**, $\mu_{eff}^2 = g^2\,[S(S+1)]$ was replaced with the effective moment for a single Co(II) with spin-orbit coupling,

$$\mu_{eff}^2 = 3\cdot\frac{a_0 + a_1\exp\left(-\frac{5}{2}Ax\right) + a_2\exp(-4Ax)}{3 + 2\exp\left(-\frac{5}{2}Ax\right) + \exp(-4Ax)}$$

$$a_0 = \frac{7}{5}(3-A)^2 + 1 + \frac{12}{25}\frac{(2+A)^2}{Ax} \qquad \text{(S3)}$$

$$a_1 = \frac{2}{45}(11-2A)^2 + \frac{176}{675}\frac{(2+A)^2}{Ax}$$

$$a_2 = \frac{1}{9}(5+A)^2 - \frac{20}{27}\frac{(2+A)^2}{Ax}$$

with $A = 3\kappa/2$, where κ is the orbital reduction coefficient that may vary between 2/3 and 1, $x = \lambda/k_BT$, where $\lambda = -\zeta/(2S)$ is the spin-orbit coupling, so for the free-ion case of Co(II), $\lambda = -(\zeta/3) = -(515/3)$ cm^{-1} = -172 cm^{-1} [2,3]. Fits were performed for compound **1**, taking A as the new parameter. These fits for both the UF and Nanjing data from compounds **1** – **3** are shown in Figure S4. The parameters obtained from these fits are given in Table S1. The resulting temperature dependence of the g-factor for **1** is shown in Figure S5. For comparative purposes, the UF data acquired on **1** was fit when $A = 0$, i.e. not including spin-orbit coupling, and the results are shown in Figure S6 for the parameters listed in Table S1.

Finally, for completeness, the possibility of zero-field splitting was considered, even though the local ligand environment does not suggest a strong effect. The data of **2** were fit to the equation appropriate for $S = 1$ dimers with zero-field splitting, D, and mean-field inter-dimer interactions

[4,5]. The results of the fits are indistinguishable (by visual inspection) from the lines shown in Figure 5, and the resulting parameters are given in Table S2. As expected on the basis of the inspection of the crystal structure, *D* is small and effectively "trades fitting weight" with the inter-dimer interaction.

Table S1. Values of the parameters obtained from fitting the Nanjing (N) and Gainesville (G) high temperature and low field data, Figure S4. The temperature dependence of the *A* parameter for the fitting of **1** are shown in Figure S5, while the results of the fit for **1** (G) with $A = 0$ are shown in Figure S6.

	1 (N)	**2 (N)**	**3 (N)**	**1 (G)**	**1 (G)**	**2 (G)**	**3 (G)**
	S = 3/2	S = 1	S = 5/2	S = 3/2	S = 3/2	S = 1	S = 5/2
g	1.95† 2.69‡	2.09	2.03	1.91† 2.60‡	2.48	2.26	1.98
J	-5.8	-5.8	-1.1	-5.3	-4.6	-5.8	-1.1
zJ′	3.0	1.6	-0.36	2.4	0.2	1.6	-0.33
ρ	0.02	0.06	0.002	0.02	0.03	0.02	0.003
χ_o	-1×10^{-4}	7×10^{-5}	-1×10^{-4}	-1×10^{-4}	0.003	8×10^{-4}	2×10^{-4}
A	1.5			1.34	0		

Each fit was performed over the entire range of the data. All *J*, *zJ′* values are stated in units of K, and all χ_o values are in units of cm^3 per mol of dimer (M_2).
† calculated from Equation S3 at $T = 2$ K; and
‡ calculated from Equation S3 at $T = 300$ K, see Figure S5.

Table S2. Values of the parameters obtained from fitting **2** for the Gainesville (G) high temperature and low field data while excluding (column repeated from Table S1) and including finite zero-field splitting, *D*. The standard "quality of fit" parameters are also listed.

	2 (G)	**2 (G)**
	$S = 1$	$S = 1$
g	2.26	2.0
J	-5.8	-4.9
zJ′	1.6	0.6
ρ	0.02	0.02
χ_o	8×10^{-4}	4×10^{-4}
D	0	0.5
Chi-sqr (fit)	2×10^{-4}	5×10^{-5}
R^2 (fit)	0.9995	0.9995

C. High temperature ac susceptibility of 1

A commercial SQUID magnetometer equipped with ac susceptibility coils was used to measure **1**, and these data, which can be contrasted to the data shown in Figure S1, are give in Figure S7.

References

1. A. Orendáčová, E. Čižmár, , L. Sedláková, J. Hanko, M. Kajňaková, M. Orendáč, A. Feher, J. S. Xia, L. Yin, D. M. Pajerowski, M. W. Meisel, V. Zeleňák, S. Zvyagin, J. Wosnitza, Phys. Rev. B **80** (2009) 144418 (8 pages) and arXiv:0906.3181.

2. O. Kahn, *Molecular Magnetism* (VCH Publishers: New York, 1993), pp 38-43.

3. B. N. Figgis and M. A. Hitchman, *Ligand Field Theory and Its Applications* (Wiley-VCH: New York, 2000), pp 107-110.

4. A. P. Ginsberg, R. L. Martin, R. W. Brookes, R. C. Sherwood, Inorg. Chem. **11** (1972) 2884-2889.

5. J. A. Schlueter, J. L. Manson, U. Geiser, Inorg. Chem. **44** (2005) 3194-3202.

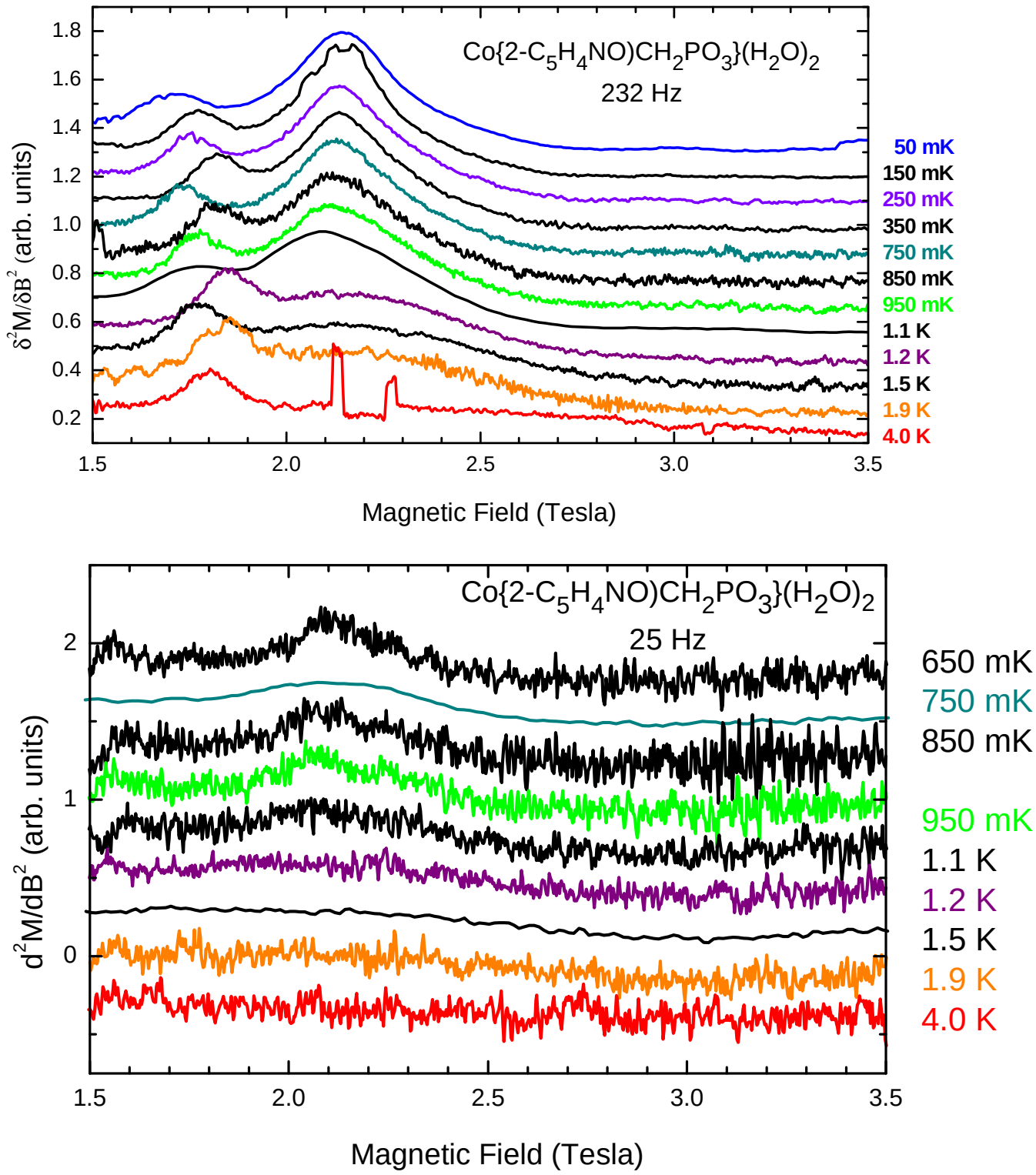

Figure S1. Isothermal data sets of **1** at 232 Hz, upper panel, and 25 Hz, lower panel.

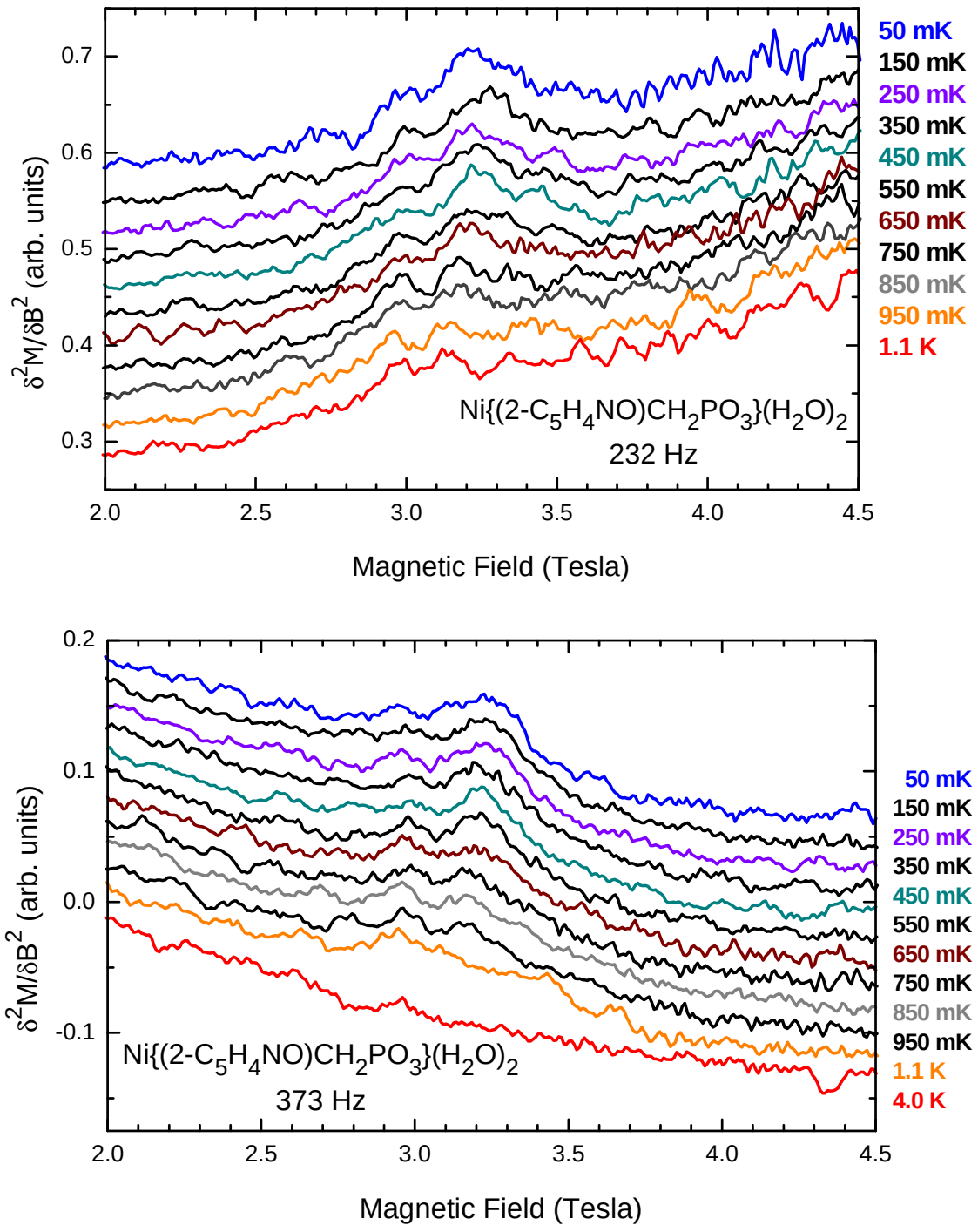

Figure S2. Isothermal data sets of **2** at 232 Hz, upper panel, and 373 Hz, lower panel.

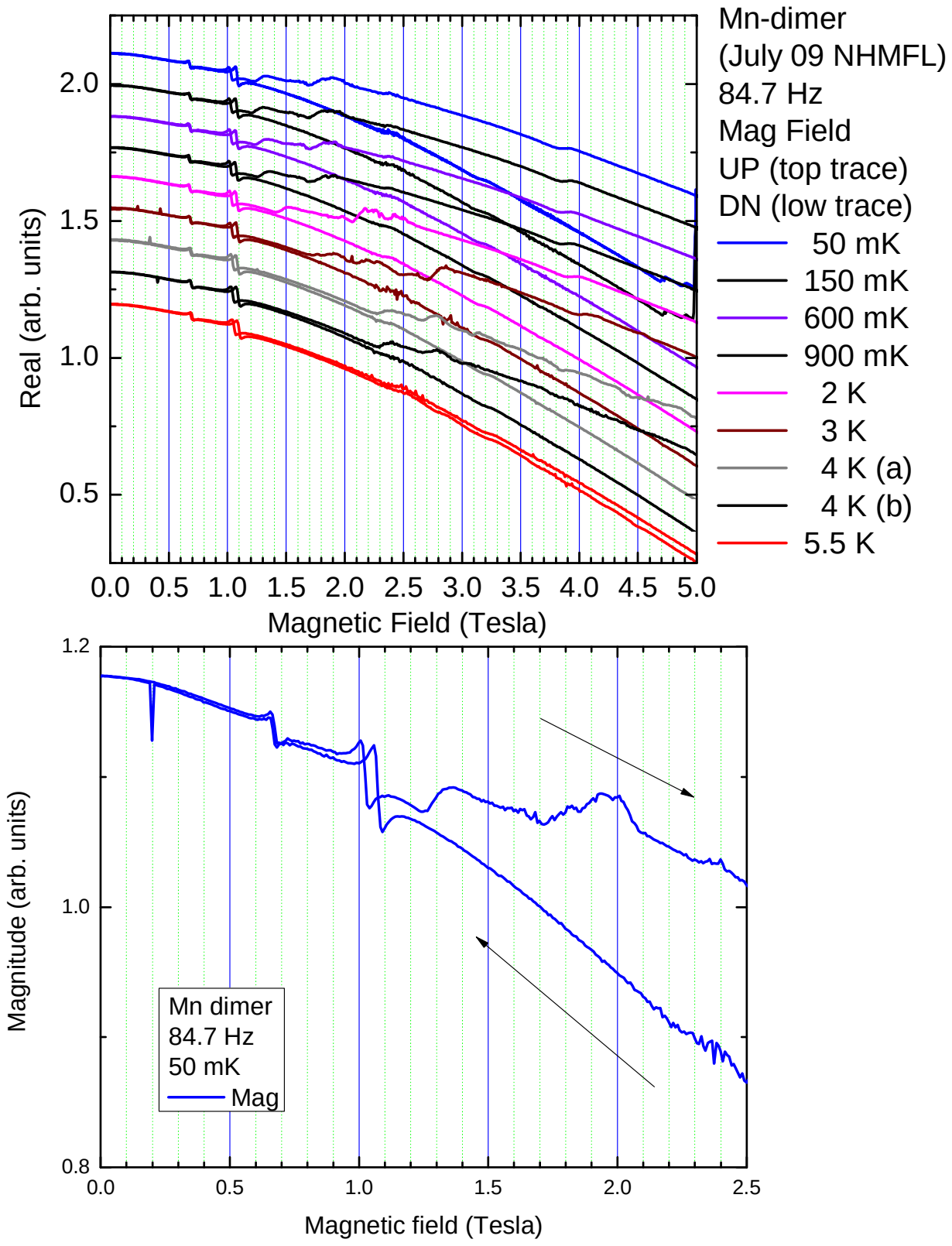

Figure S3. Isothermal data sets of **3** at 84.7 Hz for all runs, upper panel, and expanded view at 50 mK, lower panel.

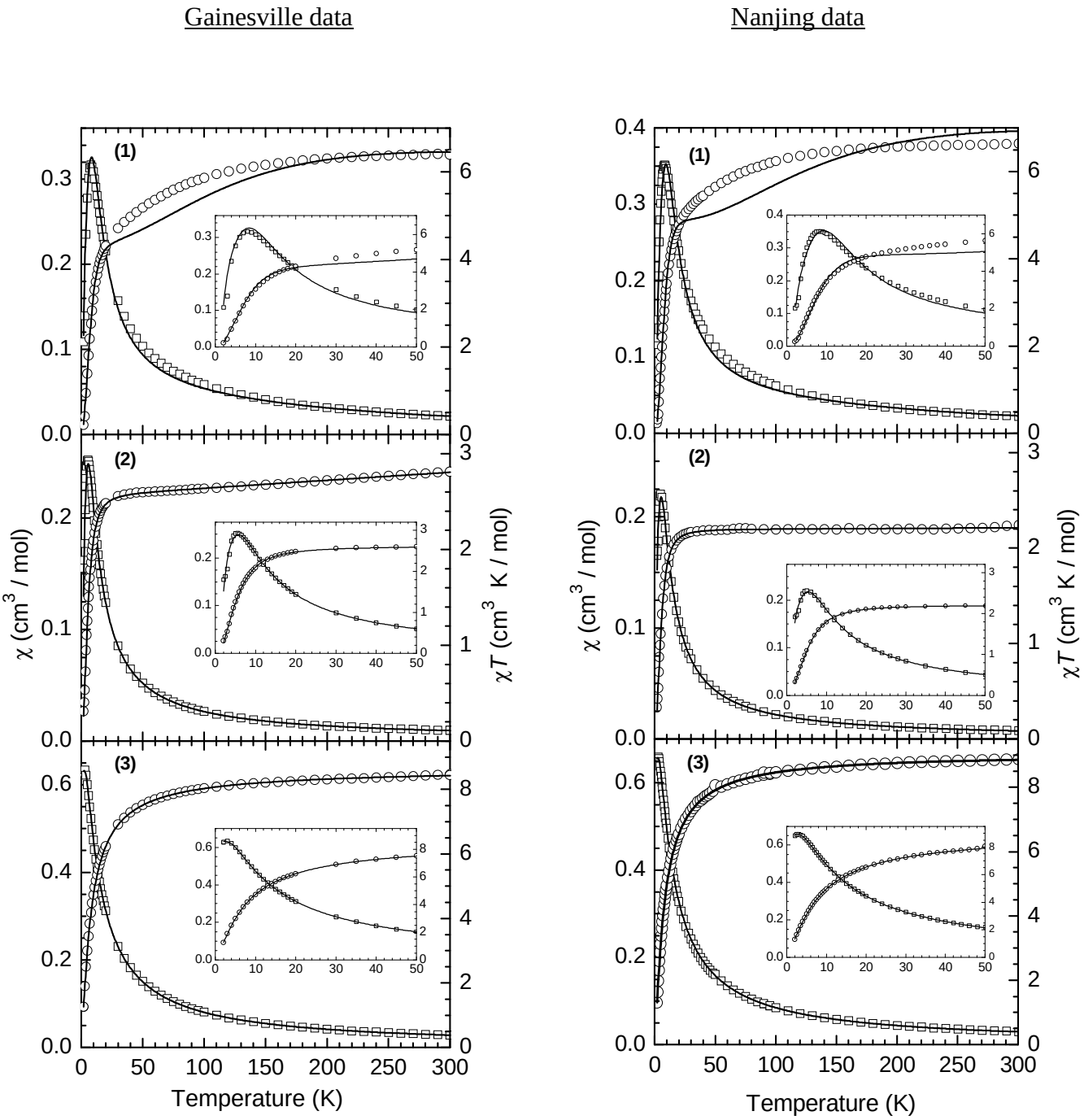

Figure S4. Data (in units of cm^3 per mol of dimer (M_2)) and fits, Equations S1-S3 and Table S1.

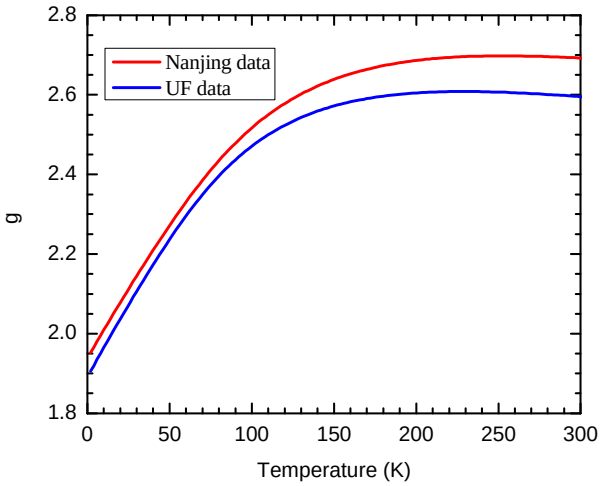

Figure S5. The *g*-value as a function of temperature, calculated using the parameters obtained from the fits described in the text.

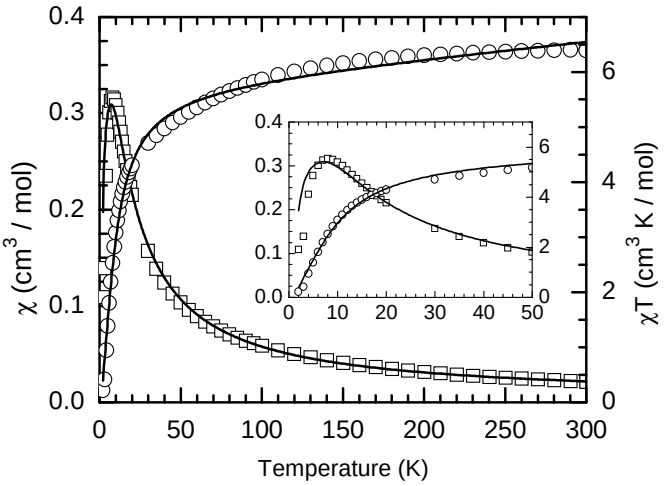

Figure S6. The data and fitting results for **1** (G) when $A = 0$.

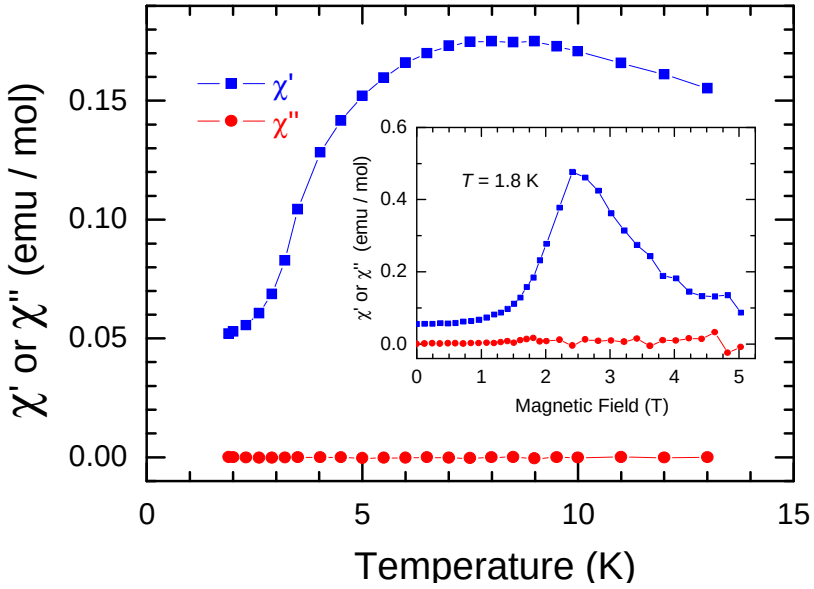

Figure S7. Temperature dependent in-phase (χ') and out-of-phase (χ'') ac magnetic susceptibilities of **1** with B_{ac} = 3 G, zero applied static magnetic field, and a frequency of 10 Hz. The inset shows the isothermal, T = 1.8 K, as a function of temperature. In all instances, the lines are connecting the data points to serve as guides for the eyes.